

# Effect of Bisphenol A on the Miscibility, Phase Morphology, and Specific Interaction in Immiscible Biodegradable Poly( $\epsilon$ -caprolactone)/Poly(L-lactide) Blends

Shiao-Wei Kuo, Chih-Feng Huang, Yi-Chih Tung, Feng-Chih Chang

*Institute of Applied Chemistry, National Chiao Tung University, Hsin Chu, Taiwan, Republic of China*

Received 14 August 2004; accepted 3 August 2005

DOI 10.1002/app.23227

Published online in Wiley InterScience (www.interscience.wiley.com).

**ABSTRACT:** We have investigated the enhancement in miscibility, upon addition of bisphenol A (BPA) of immiscible binary biodegradable blends of poly( $\epsilon$ -caprolactone) (PCL) and poly(L-lactide) (PLLA). That BPA is miscible with both PCL and PLLA was proven by the single value of  $T_g$  observed by differential scanning calorimetry (DSC) analyses over the entire range of compositions. At various compositions and temperatures, Fourier transform infrared spectroscopy confirmed that intermolecular hydrogen bonding existed between the hydroxyl group of BPA and the carbonyl groups of PCL and PLLA. The addition of BPA enhances the miscibility of the immiscible PCL/PLLA binary blend and transforms it into a miscible blend at room

temperature when a sufficient quantity of the BPA is present. In addition, optical microscopy (OM) measurements of the phase morphologies of ternary BPA/PCL/PLLA blends at different temperatures indicated an upper critical solution temperature (UCST) phase diagram, since the  $\Delta K$  effect became smaller at higher temperature (200°C) than at room temperature. An analysis of infrared spectra recorded at different temperatures correlated well with the OM analyses. © 2006 Wiley Periodicals, Inc. *J Appl Polym Sci* 100: 1146–1161, 2006

**Key words:** ternary polymer blend; hydrogen bonding; miscibility

## INTRODUCTION

During last few years, blends of biocompatible and biodegradable polymers have become attractive in polymer science because of strong economic rewards resulting from their biomedical applications.<sup>1</sup> Poly(L-lactide) (PLLA) has been studied intensively and used widely in these applications because of its high biocompatibility and good biodegradability.<sup>2,3</sup> Nonetheless, one major disadvantage of PLLA is the transition from ductile to brittle failure under tension as a result of its high melting temperature. In contrast, poly( $\epsilon$ -caprolactone) (PCL) possesses low glass transition and melting temperatures and has been added to PLLA in the role of a plasticizer to render it more flexible and to reduce its brittleness.<sup>4,5</sup> Therefore, it is reasonable to expect that blending PLLA with PCL may bring about either improved flexibility or increased strength, in comparison with the properties of each individual component. However, the phase separation in the amorphous phase has been widely observed in PLLA/

PCL blend system.<sup>6–9</sup> To enhance the compatibility of this immiscible binary PLLA/PCL blend, the mostly widely adopted strategy has been through the addition of a block copolymer, such as PLLA-*b*-PCL-*b*-PLLA,<sup>10,11</sup> PLLA-*b*-PCL,<sup>12,13</sup> or poly( $\epsilon$ -caprolactone)-*b*-poly(ethylene glycol) (PCL-*b*-PEG).<sup>14</sup> This concept arose from the early findings of Scott<sup>15</sup> and Tompa<sup>16</sup> that, if polymer B is miscible with both polymers A and C, then, it can compatibilize the immiscible binary pair of A and C. In addition to the block copolymer approach, another example of compatibilization of immiscible binary blends is through specific interactions, such as those exhibited in ternary polymer blends of poly(vinylphenol) (PVPh)/poly(methyl methacrylate) (PMMA)/poly(ethyl methacrylate) (PEMA),<sup>17</sup> and poly(vinylidene fluoride) (PVDF)/PMMA/PEMA.<sup>18</sup>

Taking into account the chemical structures of PCL and PLLA, the carbonyl groups of both PCL and PLLA are able to form intermolecular hydrogen bonds with several amorphous hydrogen-bonded donor polymers such as PVPh, phenolic, and phenoxy resins.<sup>19–23</sup> However, only partial miscibility has been observed in the PVPh/PLLA binary blend because the strength of interassociation hydrogen bonding is relatively weaker than that of the self-association hydrogen bonding of PVPh.<sup>23</sup> In addition to the use of a high-molecular-weight polymer, compatibilization of an immiscible binary polymer blend also can be achieved by blending a suitable low-molecular-weight

Correspondence to: F.-C. Chang (changfc@mail.nctu.edu.tw).

Contract grant sponsor: National Science Council, Taiwan, Republic of China; contract grant numbers: NSC-92-2216-E-009-018, NSC-92-2811-E-009-011.

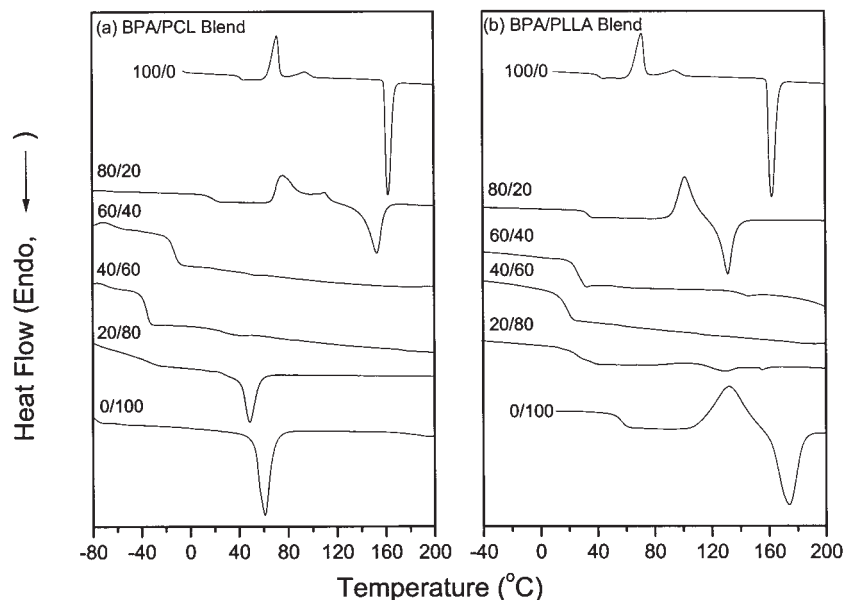


Figure 1 The DSC thermograms of (a) BPA/PCL and (b) BPA/PLLA blends having varying compositions.

(LMW) compound because of their significantly greater entropy changes relative to high-molecular-weight polymer.<sup>24</sup> Recently, He et al. reported that several bifunctional LMW compounds are miscible with PCL because of the existence of hydrogen bonds between the hydroxyl groups of dihydric phenols and the carbonyl groups of PCL. In their studies,<sup>25–31</sup> the authors also proposed that these dihydric phenols can act as compatibilizers to improve the miscibility between two hydrogen-bonding accepting polymers. As a result, LMW compound/polymer/polymer ternary blends have received considerable attention recently.<sup>32–38</sup>

In this study, we report that bisphenol A, a bifunctional, hydrogen-bond donor compound, interacts with both PCL and PLLA, which are both hydrogen-bond accepting polymers, and acts as a compatibilizer to improve their miscibility. The purpose of this work was to study the miscibility, phase morphology, and hydrogen bonding behaviors of this BPA/PCL/PLLA ternary blend system. The effect that hydrogen bonding has on the miscibility and morphology of the system was investigated using DSC, FTIR, and optical microscopy (OM).

## EXPERIMENTAL

### Materials and blend preparation

Bisphenol A, which has a molecular weight of 228 g/mol, was supplied by the Showa Chemical Company, Japan. Poly(caprolactone) (PCL) having  $M_w = 80,000$  g/mol and poly(L-lactide) (PLLA) having  $M_w = 85,000$ – $150,000$  g/mol were purchased from Aldrich Chemical Company, USA. These polymers were

used as received without further purification. The ternary blends of BPA/PCL/PLLA having various compositions were prepared by solution blending. A tetrahydrofuran (THF) solution containing 5 wt % of these three components was stirred for 6–8 h before the solution was evaporated slowly at 50°C over 1 day. The film of the blend was then dried at 100°C for 2 days to ensure total elimination of the solvent.

### Characterizations

The thermal properties of the blends were characterized using a TA Instruments 2920 differential scanning

TABLE I  
Thermal Properties of BPA/PCL and BPA/PLLA Binary Polymer Blends

	$T_g$ (°C)	$T_c$ (°C)	$\Delta H_c$ (J/g)	$T_m$ (°C)	$\Delta H_m$ (J/g)
BPA/PCL					
100/0	43	72	69	162	112
80/20	20	77 <sup>a</sup>	43	153	47
60/40	-13				
40/60	-35				
20/80	-47	-17 <sup>b</sup>	4	47	19
0/100	-62			60	70
BPA/PLLA					
100/0	43	72	69	162	112
80/20	34	102 <sup>a</sup>	55	131	52
60/40	25				
40/60	19				
20/80	25	97 <sup>c</sup>	17	135	5
0/100	57	132	94	174	102

<sup>a</sup> From the BPA phase.

<sup>b</sup> From the PCL phase.

<sup>c</sup> From the PLLA phase.

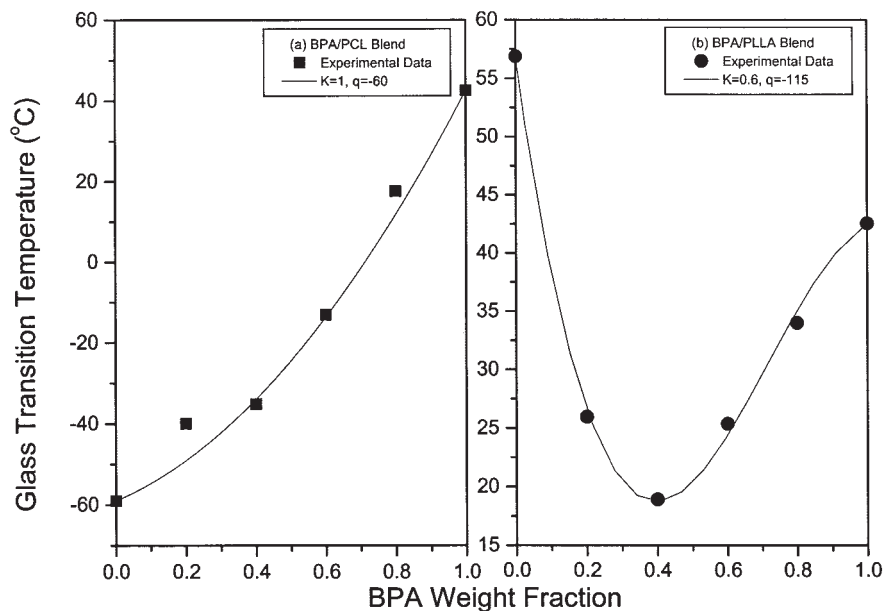


**Figure 2** Plots of  $T_g$  versus composition based on the Kwei equation for the (a) BPA/PCL and (b) BPA/PLLA blends.

calorimeter equipped with a mechanical cooling accessory. Each sample was heated to  $200^{\circ}\text{C}$ , maintained at that temperature for 5 min, and then quickly quenched to  $-100^{\circ}\text{C}$ . The glass transition and melting temperatures were obtained using a scan rate of  $20^{\circ}\text{C}/\text{min}$  within a temperature range from  $-100$  to  $200^{\circ}\text{C}$ . Infrared spectra of polymer blend films were determined by using the conventional KBr disk method. A THF solution containing the blend was cast onto a KBr disk and then dried under conditions similar to those used for the preparation of the bulk material. The

films used in this study were sufficiently thin to obey the Beer–Lambert law. FTIR spectra were recorded on a Nicolet Avatar 320 FTIR spectrophotometer from 32 scans collected at a spectral resolution of  $1\text{ cm}^{-1}$ . Because the samples containing hydroxyl groups are water-sensitive, pure nitrogen gas was used to purge the IR optical box to maintain the dryness of the sample films. IR spectra recorded at elevated temperatures were obtained by using a cell mounted inside the temperature-controlled compartment of the spectrometer. The morphologies of various blend compo-

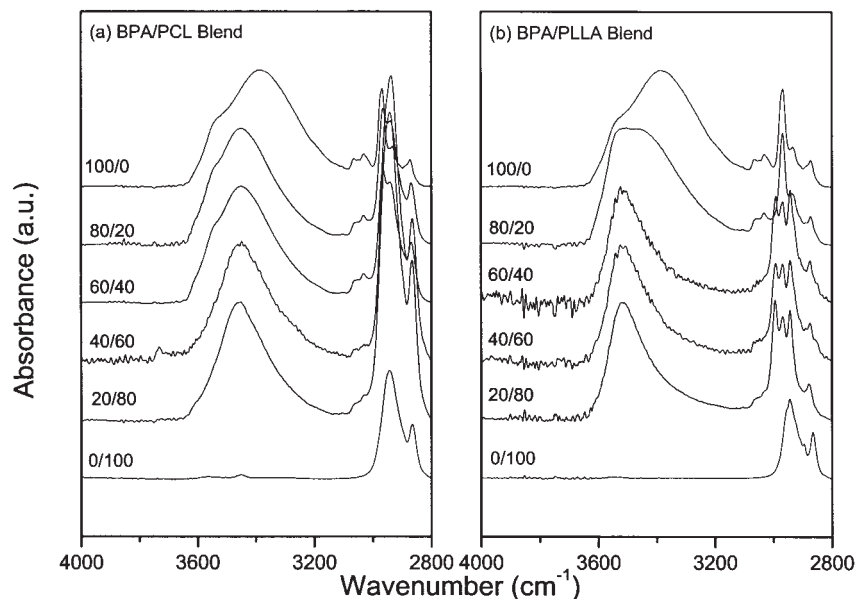


**Figure 3** The hydroxyl group stretching region of infrared spectra recorded at  $180^{\circ}\text{C}$  of the (a) BPA/PCL and (b) BPA/PLLA blends having varying compositions.

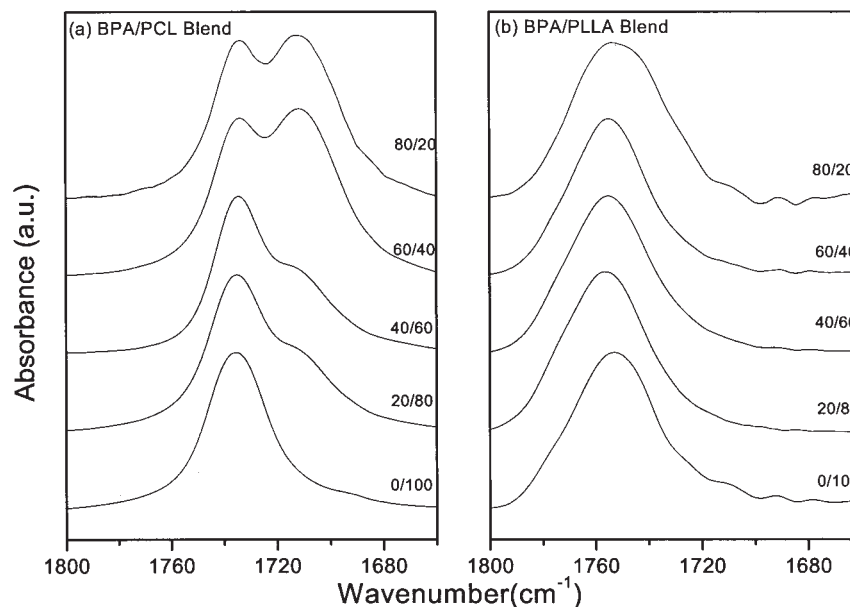


**Figure 4** The carbonyl group stretching region of infrared spectra recorded at 180°C of the (a) BPA/PCL and (b) BPA/PLLA blends having varying compositions.

sitions were observed using an Olympus BX50 microscope. A small amount of sample was sandwiched between two microscope cover slides and then heated from room temperature to 280°C at a heating rate of 10°C/min, using a Mettler Toledo FP 90 hot stage having a temperature accuracy of  $\pm 0.1^\circ\text{C}$ .

## RESULTS AND DISCUSSION

### Analyses of binary blends of BPA/polymer

#### Thermal behavior

DSC analysis is used extensively to investigate the miscibility behavior in polymer blends. At first glance, this BPA/PCL/PLLA ternary blend seems to be a

complicated one for analysis by DSC because its three components are all crystalline. For a multifunctional polymer blend system, however, the interassociation equilibrium constants of individual binary miscible pairs are expected to be different. Using the concept of competing equilibrium constants, we are able to identify the phase transitions caused by interassociation of hydroxyl-carbonyl groups or self-association of hydroxyl-hydroxyl groups. For convenience, we focus first on the thermal properties of the binary blends BPA/PCL and BPA/PLLA. Figure 1 presents the DSC curves of various compositions of BPA/PCL and BPA/PLLA blends recorded during the second heating scan. The glass transition and melting temperatures of the pure PCL are  $-60$  and  $60^\circ\text{C}$ , respectively;

**TABLE II**  
Results of Curve Fitting the FTIR Data, Recorded at 180°C, of the BPA/PCL and BPA/PLLA Binary Blends

	Free C=O			Bonded C=O			$f_b$ (%)
	$\nu$ ( $\text{cm}^{-1}$ )	$W_{1/2}$ ( $\text{cm}^{-1}$ )	$A_f$ (%)	$\nu$ ( $\text{cm}^{-1}$ )	$W_{1/2}$ ( $\text{cm}^{-1}$ )	$A_f$ (%)	
<b>BPA/PCL</b>							
0/100	1735	27	100	—	—	—	0
20/80	1735	26	66	1709	28	34	26.4
40/60	1736	23	65	1709	28	35	26.6
60/40	1737	20	34	1710	29	66	57.0
80/20	1737	19	32	1711	30	68	58.7
<b>BPA/PLLA</b>							
0/100	1757	32	100	—	—	—	—
20/80	1756	33	100	—	—	—	—
40/60	1755	33	100	—	—	—	—
60/40	1754	34	100	—	—	—	—
80/20	1751	36	100	—	—	—	—

**TABLE III**  
**Summary of the Self-Association and Interassociation Equilibrium Constants and Thermodynamic Parameters for the BPA/PCL/PLLA Ternary Blends at Room Temperature**

Polymer	Molar volume (mL/mol)	Molecular weight (g/mol)	Solubility parameter (cal/mL) <sup>0.5</sup>	Self-association equilibrium constant and enthalpy		Interassociation equilibrium constant and enthalpy	
				$K_B$	$h_B$	$K_A$	$h_A$
BPA <sup>a</sup>	176.6	228.3	10.38	66.8 <sup>b</sup>	-5.2 <sup>b</sup>		
PCL <sup>a</sup>	107	114	9.21			90.1 <sup>c</sup>	-4.2 <sup>c</sup>
PLLA <sup>a</sup>	69.8	86.1	9.61			10.0 <sup>d</sup>	-3.0 <sup>e</sup>

<sup>a</sup> The molar volume, molecular weight, and solubility parameter are estimated by using a group contribution method proposed by Kwei et al.<sup>18, b18, c12, d12</sup>; and <sup>e</sup>estimated by using the  $\Delta\nu$ .<sup>18</sup>

the corresponding temperatures for pure PLLA are 57 and 174°C, respectively. Interestingly, even though the molar mass of bisphenol A is only 228 g/mol, it also shows a single  $T_g$  behavior at 43°C during the second heating scan. BPA contains a high density of hydroxyl groups, which probably results in the formation of a weakly noncovalently crosslinked supramolecular network. In addition, pure BPA has a melting temperature of 162°C, which we have discussed in a previous study.<sup>32</sup> Both binary blends, BPA/PCL and BPA/PLLA, are totally miscible in the amorphous phase based on single values of  $T_g$  detected by DSC analyses, as displayed in Figure 1; their related thermal properties are summarized in Table I. Meanwhile, the melting temperatures of PCL and PLLA also shift gradually to lower temperatures upon increasing the content of BPA. A depression in the melting temperature is characteristic of a miscible polymer blend in melting state. In the BPA/PCL blend system, the value of  $T_g$  of the blend increases upon increasing the BPA content, but it decreases in the BPA/PLLA blend.

Furthermore, the value of  $T_g$  in the BPA/PLLA blend is lower than that of both the individual components, since intermolecular hydrogen bonding is expected to destroy the crystalline phases of both BPA and PLLA, as is indicated in Figure 1(b). Thus, the small molecule can act as a plasticizer and reduce the value of  $T_g$  of these components. Generally, the Kwei eq. (1)<sup>39</sup> has been used widely to predict the variation of the glass transition temperature as a function of the composition of a miscible blend that exhibits hydrogen bonding.

$$T_g = \frac{W_1 T_{g1} + kW_2 T_{g2}}{W_1 + kW_2} + qW_1 W_2 \quad (1)$$

where  $W_1$  and  $W_2$  are the weight fractions of the compositions, and  $T_{g1}$  and  $T_{g2}$  represent the corresponding glass transition temperatures. The fitting constants  $k$  and  $q$  are parameters corresponding to the strength of hydrogen bonding in the blend. Figure 2

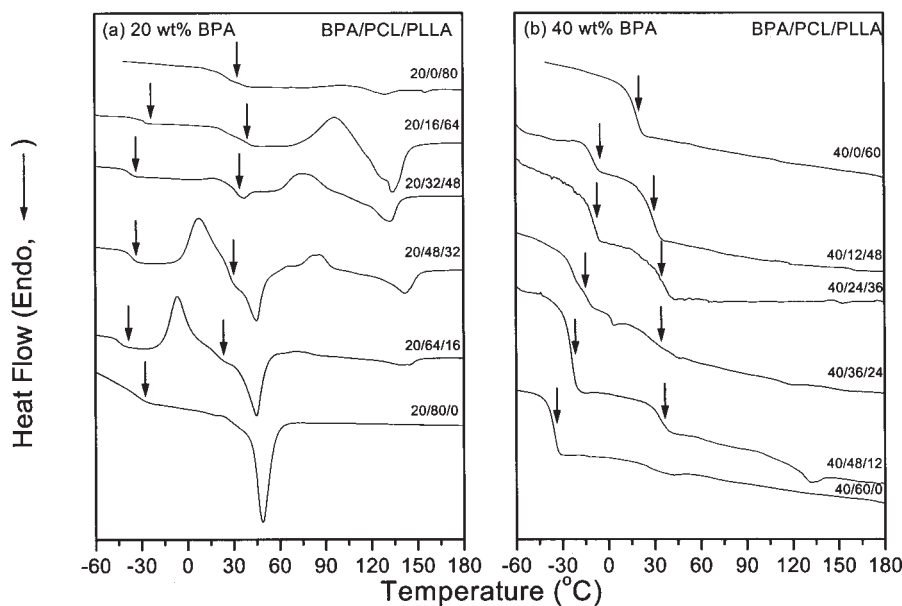


**Figure 5** DSC thermograms of BPA/PCL/PLLA ternary blends having varying compositions (BPA content: 20 or 40 wt %).

TABLE IV  
Thermal Properties of BPA/PCL/PLLA Ternary  
Polymer Blends

BPA/PCL/PLLA	$T_g$ (°C)	$T_c$ (°C)	$\Delta H_c$ (J/g)	$T_m$ (°C)	$\Delta H_m$ (J/g)	
	-44 <sup>ab</sup>	19 <sup>ac</sup>	-6 <sup>b</sup>	29	45	41
20/64/16			70 <sup>c</sup>	6	140	8
	-36	27	8 <sup>b</sup>	21	46	27
20/48/32			87 <sup>c</sup>	6	142	13
20/32/48	-37	32	74 <sup>c</sup>	15	132	21
20/16/64	-28	27			134	19
40/48/12	-24	33				
40/36/24	-23	26				
40/24/36	-10	38				
40/12/48	-9	30				
60/32/8	7	26				
60/24/16	0	21				
60/16/24	13	32				
60/8/32	16	33				
80/16/4	37 <sup>abc</sup>	83 <sup>a</sup>	60	156	74	
80/12/8	26	97 <sup>a</sup>	52	151	60	
80/8/12	31	96 <sup>a</sup>	49	153	54	
80/4/16	18					

<sup>a</sup> From the BPA phase.

<sup>b</sup> From the PCL phase.

<sup>c</sup> From the PLLA.

<sup>ab</sup> From the BPA-PCL phases.

<sup>ac</sup> From the BPA-PLLA phases.

<sup>abc</sup> BPA-PCL-PLLA phases.

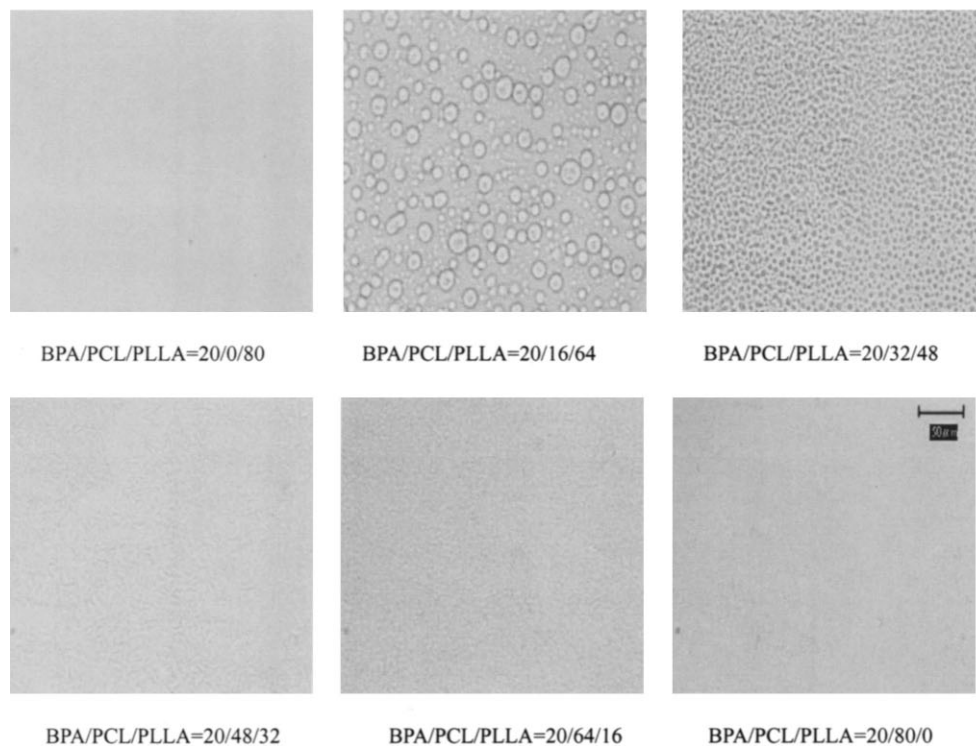
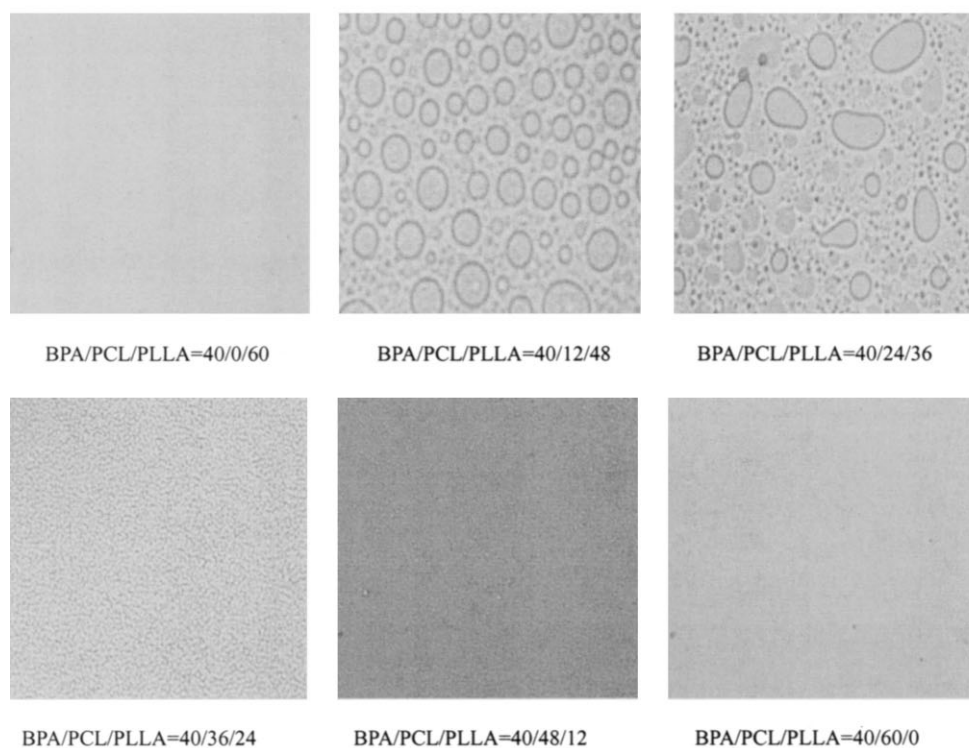
shows the dependence of the value of  $T_g$  on the composition of the miscible BPA/PCL and BPA/PLLA blends, where  $k = 1$  and  $q = -85$  for the former blend and  $k = 0.6$  and  $q = -100$  for the latter. Negative deviations were also observed in many previous studies.<sup>40-42</sup> The fact that both of the values of  $q$  are negative indicates that the self-associated hydrogen-bonded structure of BPA is broken to form weaker interassociated hydrogen bonds. According to the values of  $k$  and  $q$  obtained experimentally in this study, the interassociation hydrogen bonding in the BPA/PCL blend is greater than that in the BPA/PLLA blend. To support this claim, we turned our attention next to FTIR analyses.

#### FTIR analyses

FTIR spectroscopy is a useful technique for investigating the strength of hydrogen bonding between different molecules. Figure 3 shows the FTIR spectra of the BPA/PCL and BPA/PLLA blends in the regions of the hydroxyl group vibrations; the spectra were obtained using blends having varying BPA fractions and were recorded at 180°C (i.e., above the melting temperatures of these three components). Pure BPA exhibits a broad band centered at 3383  $\text{cm}^{-1}$ , which we attribute to the wide distribution of hydrogen-bonded hydroxyl groups. A small and narrow band at 3525  $\text{cm}^{-1}$  results from free hydroxyl groups. The broad hydrogen-bonded hydroxyl band shifts to higher wave numbers

upon increasing both the PCL and PLLA contents, with the wave numbers for samples having 20 wt % BPA at 3450 and 3520  $\text{cm}^{-1}$  for PCL and PLLA, respectively. This shift reflects a new distribution of hydrogen bonds, i.e., specific hydroxyl-hydroxyl and hydroxyl-carbonyl interactions. In general, the frequency difference between a hydrogen-bonded hydroxyl absorption and the free hydroxyl absorption ( $\Delta\nu$ ) allows a rough estimate to be made of the average hydrogen bonding strength and its enthalpy in hydrogen-bonded blend systems.<sup>43</sup> Thus, all these observed changes arise from switching the strong self-association mediated by hydroxyl-hydroxyl bonds into the relatively weaker intermolecular hydroxyl-carbonyl bonds of the BPA/PCL and BPA/PLLA blends. From analysis of these spectra, the average strengths of the hydrogen bonds for either the self-association of the hydroxyl groups of BPA or its interassociation with the carbonyl groups of PCL and PLLA increases in the order BPA/BPA ( $\Delta\nu = 142 \text{ cm}^{-1}$ ) > BPA/PCL ( $\Delta\nu = 75 \text{ cm}^{-1}$ ) > BPA/PLLA ( $\Delta\nu = 5 \text{ cm}^{-1}$ ). All these results are consistent with the negative values of  $q$  obtained using the Kwei equation. Figure 4 shows the corresponding region of the carbonyl group vibration in the FTIR spectra recorded at 180°C of the BPA/PCL and BPA/PLLA blends in which the BPA fractions were varied. Both pure PCL and PLLA exhibit a carbonyl vibration band centered at 1734 and 1756  $\text{cm}^{-1}$ , respectively, that corresponds to the free carbonyl group. On increasing the BPA content of the BPA/



**(a): 20 wt% BPA****(b): 40 wt% BPA**

**Figure 6** Optical micrographs recorded at 40°C of BPA/PCL/PLLA ternary blends having varying compositions. BPA content: (a) 20 wt % and (b) 40 wt %.

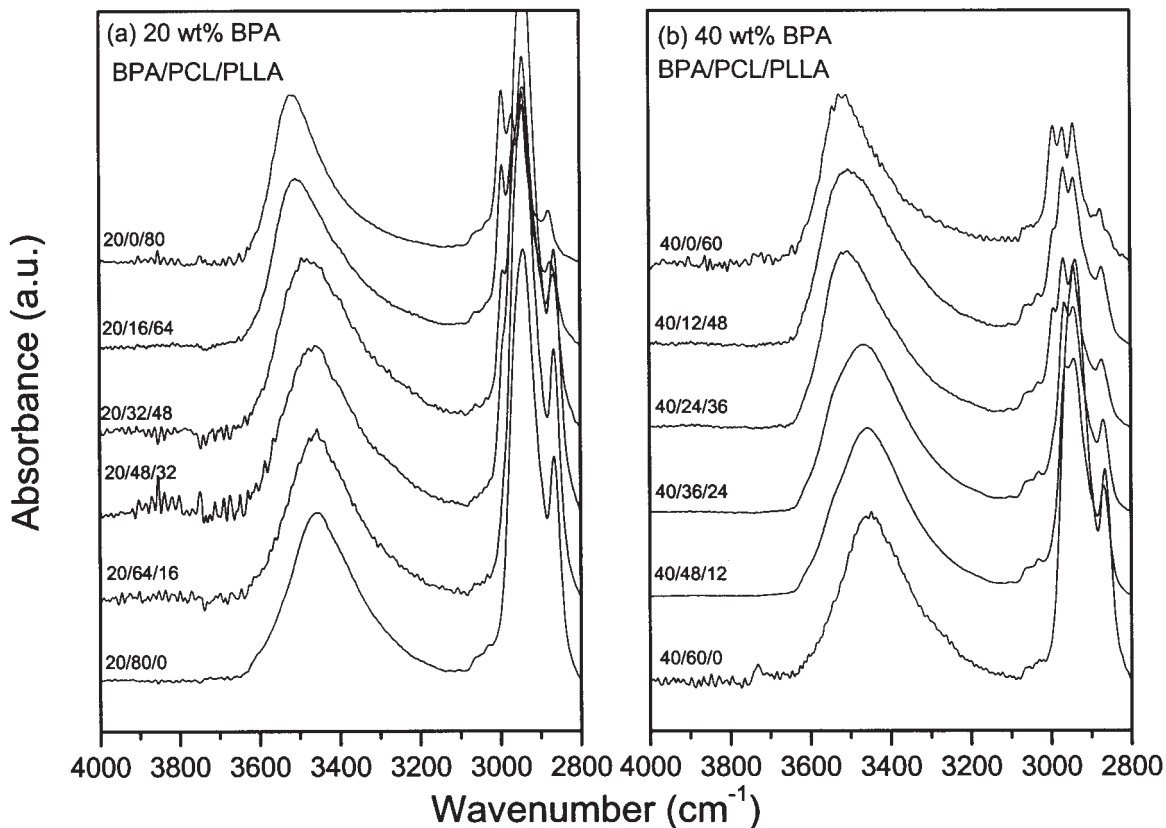


**Figure 7** The hydroxyl group stretching region of infrared spectra recorded at 180°C of BPA/PCL/PLLA ternary blends containing a constant composition of BPA: (a) 20 wt % and (b) 40 wt %.

PCL blend system, a second band appears at a lower wave number ( $1710\text{ cm}^{-1}$ ), which we attribute to vibration of the hydrogen-bonded carbonyl groups.

These two bands representing the groups can be fitted well to the Gaussian function. The fraction of the hydrogen-bonded carbonyl group can be calculated

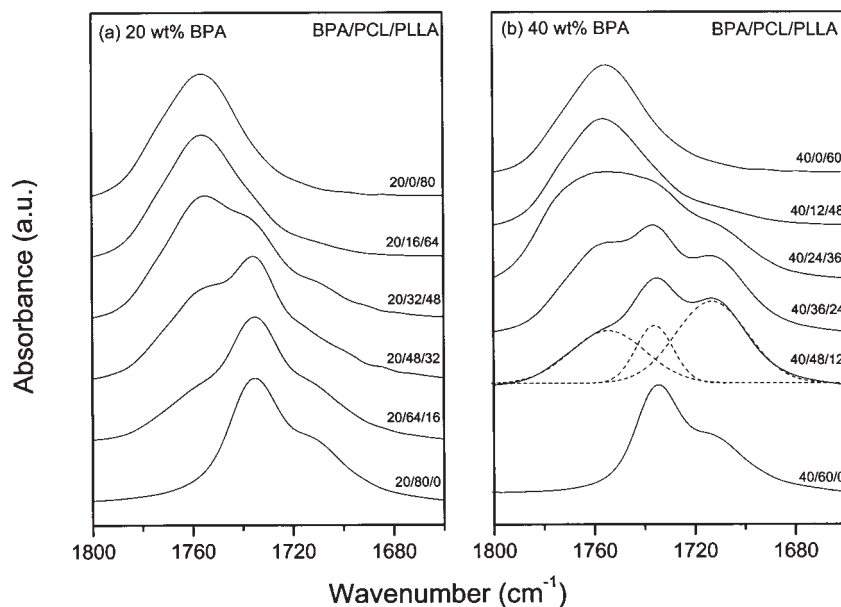


**Figure 8** The carbonyl group region of infrared spectra recorded at 180°C of ternary blend of BPA/PCL/PLLA containing constant composition of BPA: (a) 20 wt % and (b) 40 wt %.



TABLE V  
Results of Curve Fitting the FTIR Data Recorded at 180°C Results for the BPA/PCL/PLLA Ternary Blends

BPA/PCL/PLLA	PCL						PLLA			$f_b$ (%)
	Free C=O			Bonded C=O			Free C=O			
	$\nu$ (cm <sup>-1</sup> )	$W_{1/2}$ (cm <sup>-1</sup> )	$A_f$ (%)	$\nu$ (cm <sup>-1</sup> )	$W_{1/2}$ (cm <sup>-1</sup> )	$A_f$ (%)	$\nu$ (cm <sup>-1</sup> )	$W_{1/2}$ (cm <sup>-1</sup> )	$A_f$ (%)	
20/64/16	1736	16	32	1722	30	45	1756	30	23	48.7
20/48/32	1735	13	19	1722	32	35	1755	31	46	54.8
20/32/48	1734	12	5	1723	35	31	1756	31	64	80.9
20/16/64	1733	10	1	1720	31	12	1756	32	87	86.0
40/48/12	1736	14	15	1713	30	50	1754	32	35	69.3
40/36/24	1736	13	11	1714	30	40	1756	31	49	71.4
40/24/36	1738	15	18	1709	30	22	1758	30	60	63.4
40/12/48	1738	15	7	1719	37	18	1758	30	75	44.8
60/32/8	1736	15	11	1711	34	58	1757	30	31	77.5
60/24/16	1736	14	11	1713	30	39	1756	31	48	67.0
60/16/24	1737	16	13	1712	30	36	1757	29	51	65.0
60/8/32	1737	17	15	1714	29	23	1758	29	62	51.0
80/16/4	1736	15	10	1710	25	49	1754	29	41	75.7
80/12/8	1736	14	10	1710	28	46	1755	29	44	71.1
80/8/12	1737	15	11	1710	27	39	1755	29	50	68.5
80/4/16	1736	14	12	1710	27	38	1754	29	50	67.5

using the absorptivities ratio ( $a = a_{\text{HB}}/a_F = 1.5$ ) in accord with previous studies of infrared spectra of systems undergoing hydroxyl-carbonyl interassociation.<sup>44</sup> Table II summarizes the results from curve fitting and indicates that the fraction of hydrogen-bonded carbonyl groups increases upon increasing the BPA content. In contrast, the hydrogen-bonding interaction between BPA and PLLA is not strong, since we observed no significant shift in the wave number of the carbonyl group for the BPA/PLLA blends that was also observed in PVPh/PLLA blend.<sup>22</sup> Only the half-width of the signal of the free PLLA carbonyl

groups is increased and its wave number shifts by 5 cm<sup>-1</sup> when blended with BPA at 80 wt %. Table II also summarizes the results of curve fitting these shifts to the Gaussian function. Our results appear to be consistent with the inter- and self-association equilibrium constants obtained for the PVPh/PCL and PVPh/PLLA blend systems based on the Painter-Coleman association model (Table III). The value of the self-association equilibrium constant ( $K_B$ ) for PVPh is 66.8 at 25°C, and the values of the interassociation equilibrium constants ( $K_A$ ) for the PVPh/PCL and PVPh/PLLA blend systems are 90.1 and 10.0, previously.<sup>19,21</sup>

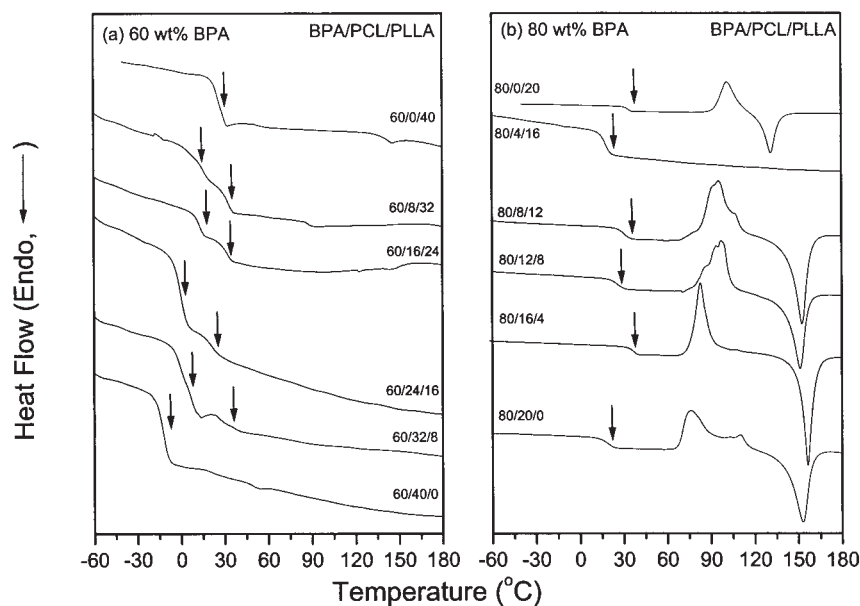
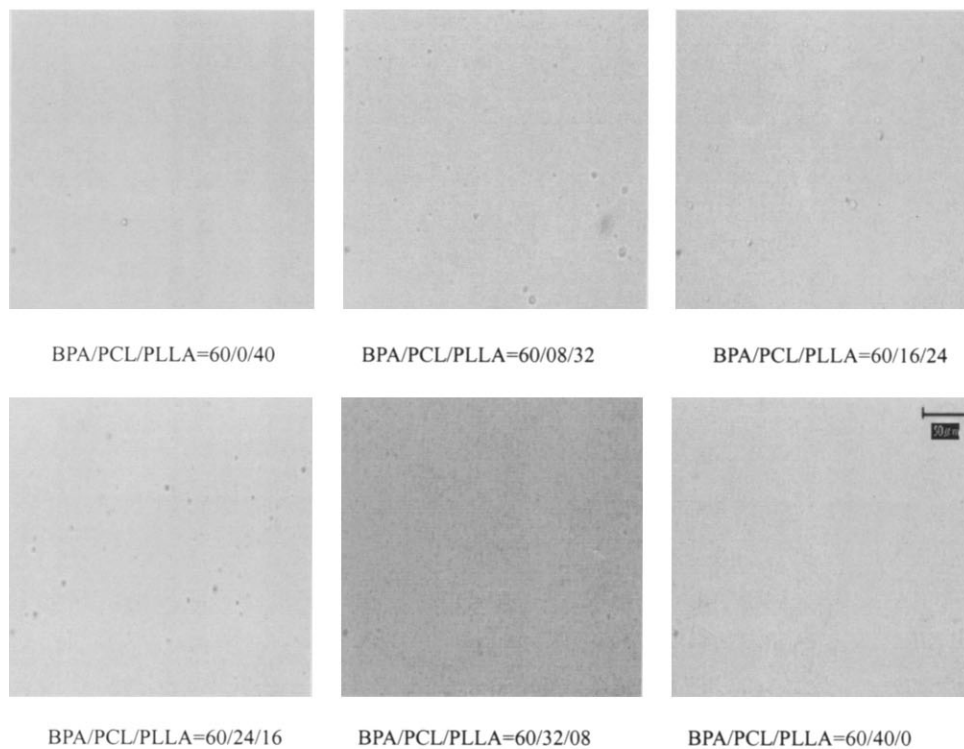
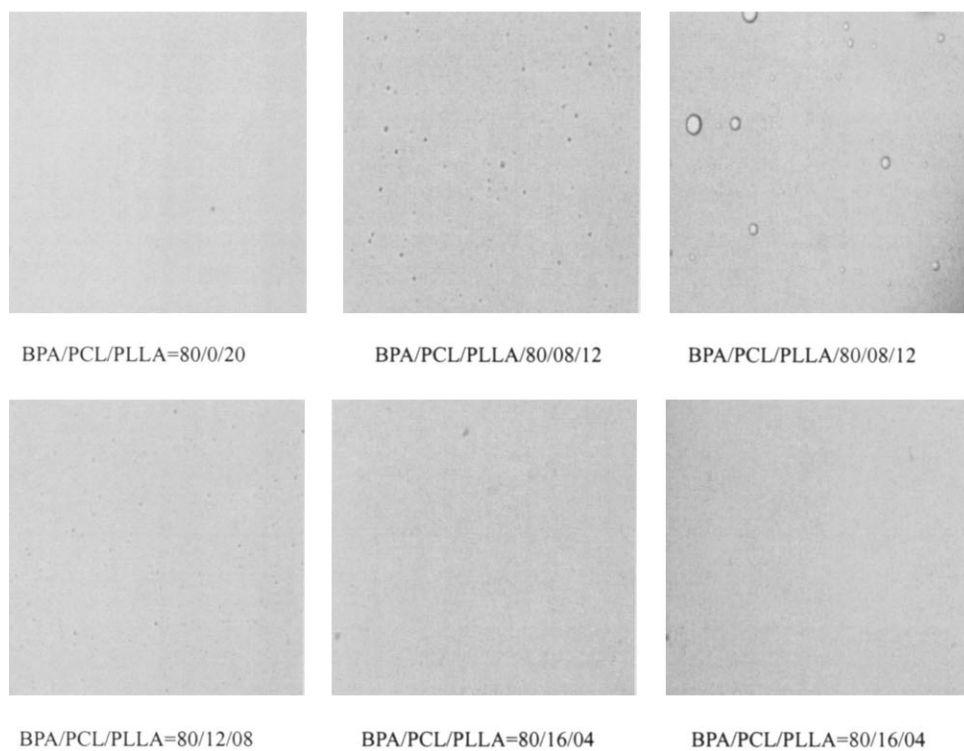


Figure 9 DSC thermograms of BPA/PCL/PLLA ternary blends having varying BPA content: (a) 60 wt % and (b) 80 wt %.

## (a) 60 wt% BPA



## (b) 80 wt% BPA



**Figure 10** Optical micrographs recorded at 40°C of BPA/PCL/PLLA ternary blends having varying BPA content: (a) 60 wt % and (b) 80 wt %.

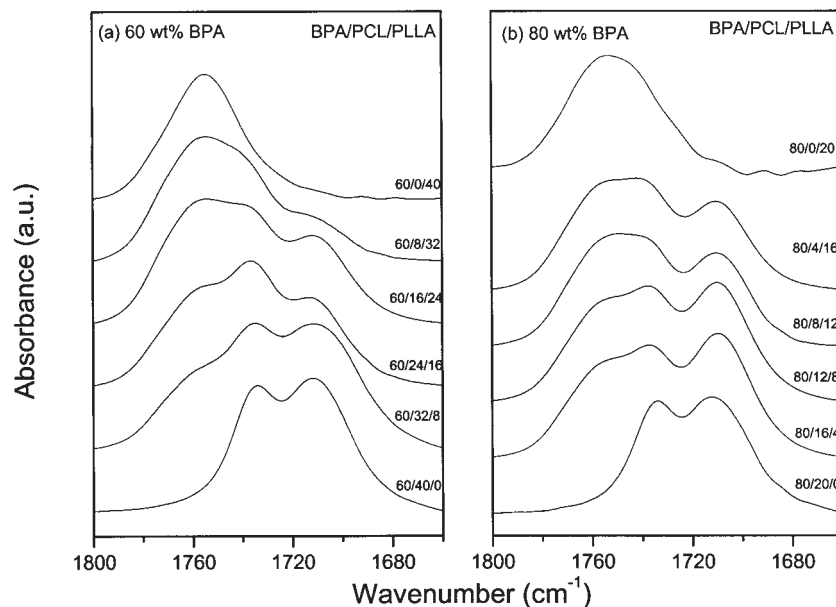


**Figure 11** The carbonyl group region of infrared spectra recorded at 180°C of ternary blend of BPA/PCL/PLLA containing constant composition of BPA: (a) 60 wt % and (b) 80 wt %.

It is apparent that these results, from both theoretical predictions and experimental observations, indicate that the interassociation hydrogen bonding between phenolic-hydroxyl groups and PCL's carbonyl is indeed stronger than that between phenolic-hydroxyl groups and PLLA's carbonyl from. In addition, the ratio  $K_A/K_B$  for the PLLA/BPA system is quite small, indicating that the hydroxyl-carbonyl hydrogen-bonding of PLLA is insignificant.

#### Bisphenol A/PCL/PLLA ternary blends

Figure 5 shows second-run DSC curves of BPA/PCL/PLLA ternary blends containing a constant BPA content [(a) 20 wt %; (b) 40 wt %] and various PCL/PLLA ratios (80:20, 60:40, 40:60, and 20:80). Table IV summarizes the thermal properties of these systems. Although both the BPA/PCL and BPA/PLLA binary blends exhibit a single value of  $T_g$ , all the BPA/PCL/PLLA ternary blends containing 20 and 40 wt % of BPA have two values of  $T_g$ , which implies that their components are immiscible in the amorphous phase. In general, the phase separation in a ternary blend is caused by the difference in the physical interactions between BPA/PCL and BPA/PLLA. In addition, the difference in interassociation equilibrium constant between BPA/PCL and BPA/PLLA blend systems also tends to induce phase separation.<sup>45-47</sup> Although the physical interaction ( $\Delta\chi$  effect) is favored in the BPA/PLLA blend (smaller solubility parameter difference), BPA interacts more favorably with PCL than it does with PLLA, which is defined as a  $\Delta K$  effect (chemical interaction). In general, the  $\Delta K$  effect is more domi-

nant than the effect in a ternary blend system. Clearly, the melting temperature and enthalpy of the PLLA phase increase upon the addition of PCL into the BPA/PLLA binary blend, such as we observe in Figures 5(a) and 5(b) for the blends having BPA/PCL/PLLA = 20/16/64 and 40/48/12. This phenomenon arises from the weaker hydroxyl-carbonyl interassociation of BPA/PLLA gradually breaking down upon increasing the PCL content in these ternary blends. As a result, the PLLA become excluded from the miscible system to form its own domain and crystallization occurs. Therefore, these BPA/PCL/PLLA ternary blends containing relatively low BPA content (20 or 40 wt %) have two values of  $T_g$ . The higher and lower glass transitions temperatures represent the BPA-PLLA and BPA-PCL phases, respectively. We emphasize that the value of  $T_g$  of the BPA-PLLA phase in Figure 5(a) at higher PCL content overlaps slightly with the melting temperature of the PCL phase. To further confirm that phase separation indeed occurs in this ternary blend, we turned our attention next to analyses by OM.

Figure 6 shows optical micrographs of BPA/PCL/PLLA blends at constant BPA content (20 and 40 wt %). As we see in these photographs, all of these ternary blends are heterogeneous, while all of the binary blends are homogeneous. Clearly, the phase separation domain size decreases with increasing of the PCL content as a result of the average hydrogen bonding strength increasing accordingly, which is confirmed by FTIR spectra. Figure 7 shows the regions of the hydroxyl group vibrations in the FTIR spectra obtained at 180°C for BPA/PCL/PLLA blends having

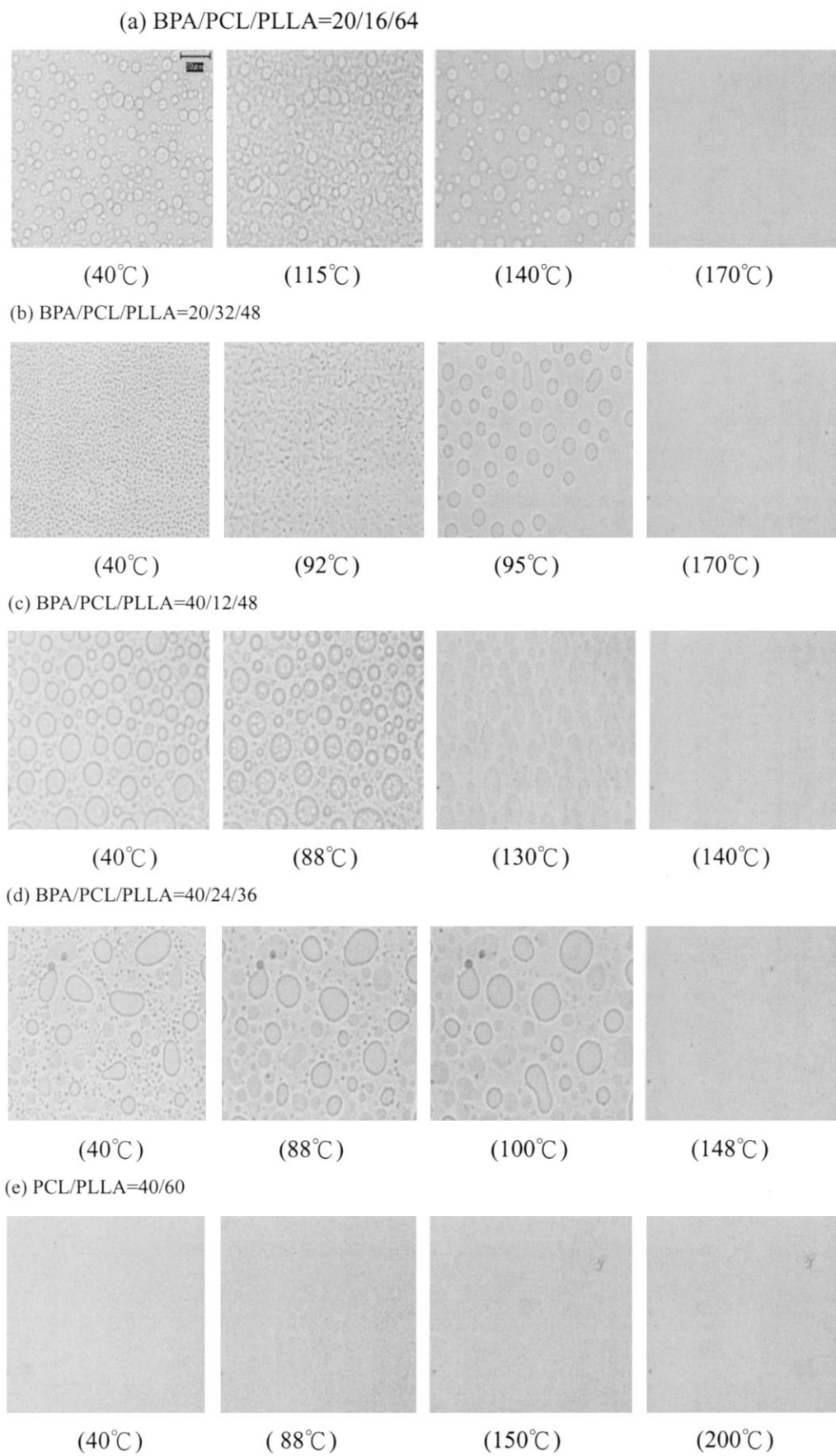


**Figure 12** Optical micrographs recorded at various temperatures of BPA/PCL/PLLA ternary blends having selected compositions.

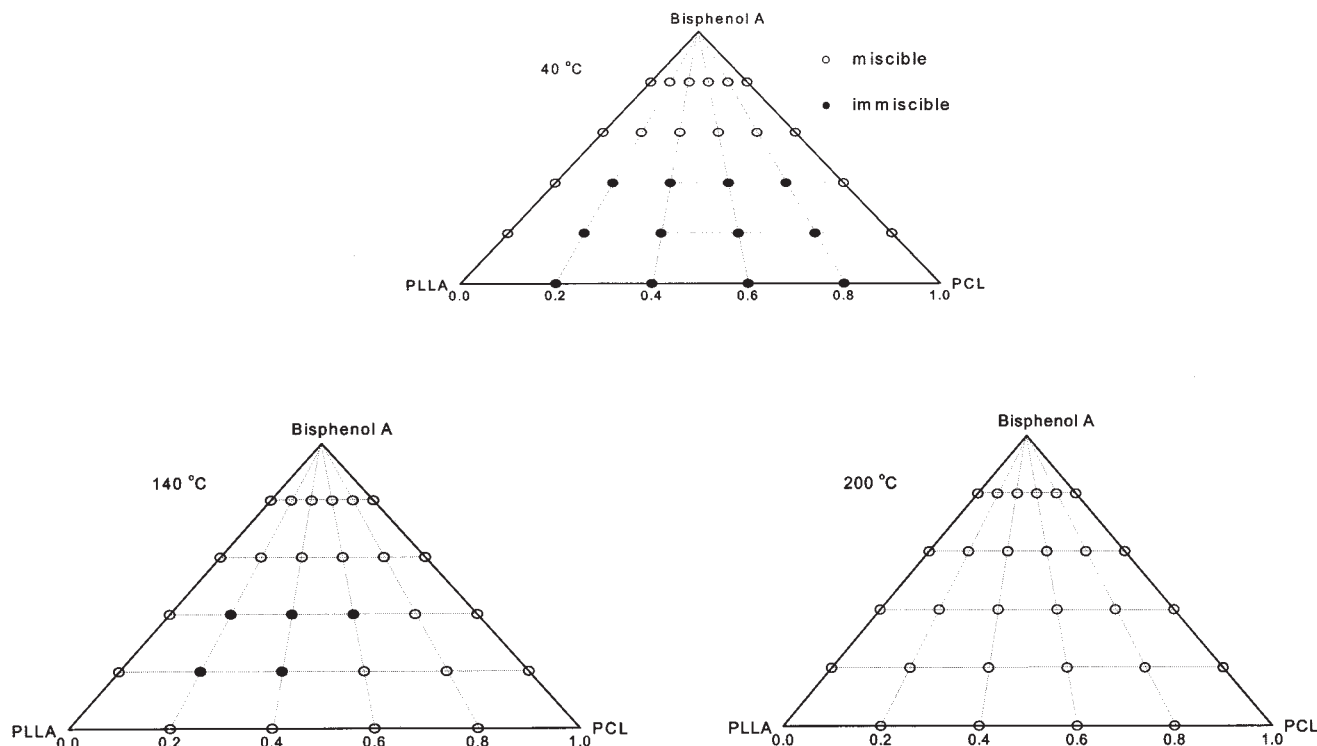


**Figure 13** Ternary phase diagram of the BPA/PCL/PLLA system at (a) 40, (b) 140, and (c) 200°C. The open circles represent miscible ternary blends and the full circles represent immiscible ternary blends.

constant BPA (20 or 40 wt %) and varying PCL content. Clearly, the signal of the hydrogen-bonded hydroxyl group of the BPA/PLLA system shifts to lower wave number with increasing PCL content, indicating that the average strength of hydrogen bonding increases during this process. Figure 8 presents the carbonyl stretching region ( $1660\text{--}1800\text{ cm}^{-1}$ ) of the infrared spectra of these ternary blends measured at 180°C. Three major absorptions are observed for stretching of the carbonyl groups. As mentioned earlier, we attribute the vibration bands centered at 1734 and 1756

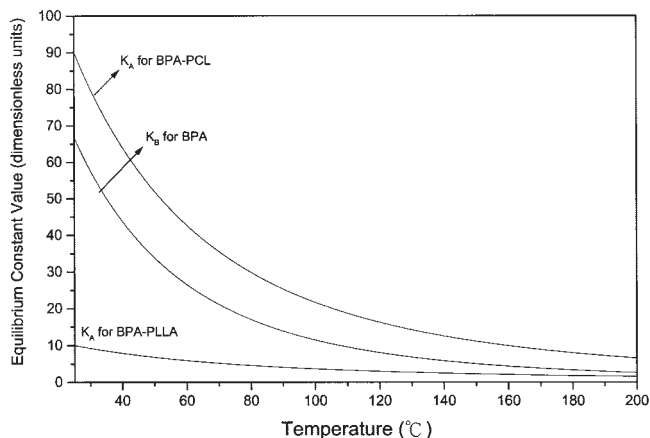


**Figure 14** Values of equilibrium constants as a function of temperature between 25 and 200°C.

$\text{cm}^{-1}$  to the free carbonyl groups of PCL and PLLA, respectively. We attribute the third band at  $1710\text{ cm}^{-1}$  to the vibration of the hydrogen-bonded carbonyl groups of PCL. These three bands also can be fitted well to a Gaussian function, as presented in Figure 8(b), and Table V summarizes the results of this curve fitting. At lower BPA content (20 wt %), the fraction of PCL's hydrogen-bonded carbonyl group increases by increasing the PLLA content, which indicates that the hydroxyl groups of BPA prefer interacting with the carbonyl groups of PCL and, thus, the PLLA phase separates from the miscible BPA/PCL phase. However, at higher BPA content (40 wt %), the fraction of hydrogen-bonded carbonyl group of PCL increases initially and then decreases with further increase of the PLLA content, because a portion of the hydroxyl groups of BPA begins to interact with the carbonyl group of the PLLA. As a result, the fraction of hydrogen-bonded carbonyl groups of PCL decreases at higher PLLA content.

Figure 9 shows the conventional second-run DSC curves of BPA/PCL/PLLA ternary blends containing a higher constant composition of BPA [(a) 60 wt %; (b) 80 wt %]; Table IV also summarizes their related thermal properties. Clearly, single values of  $T_g$  are observed for the ternary blend having a BPA content of 80 wt %, which strongly suggests that these blends are fully miscible and have a homogeneous amorphous phase. Furthermore, the recrystallization and melting temperatures



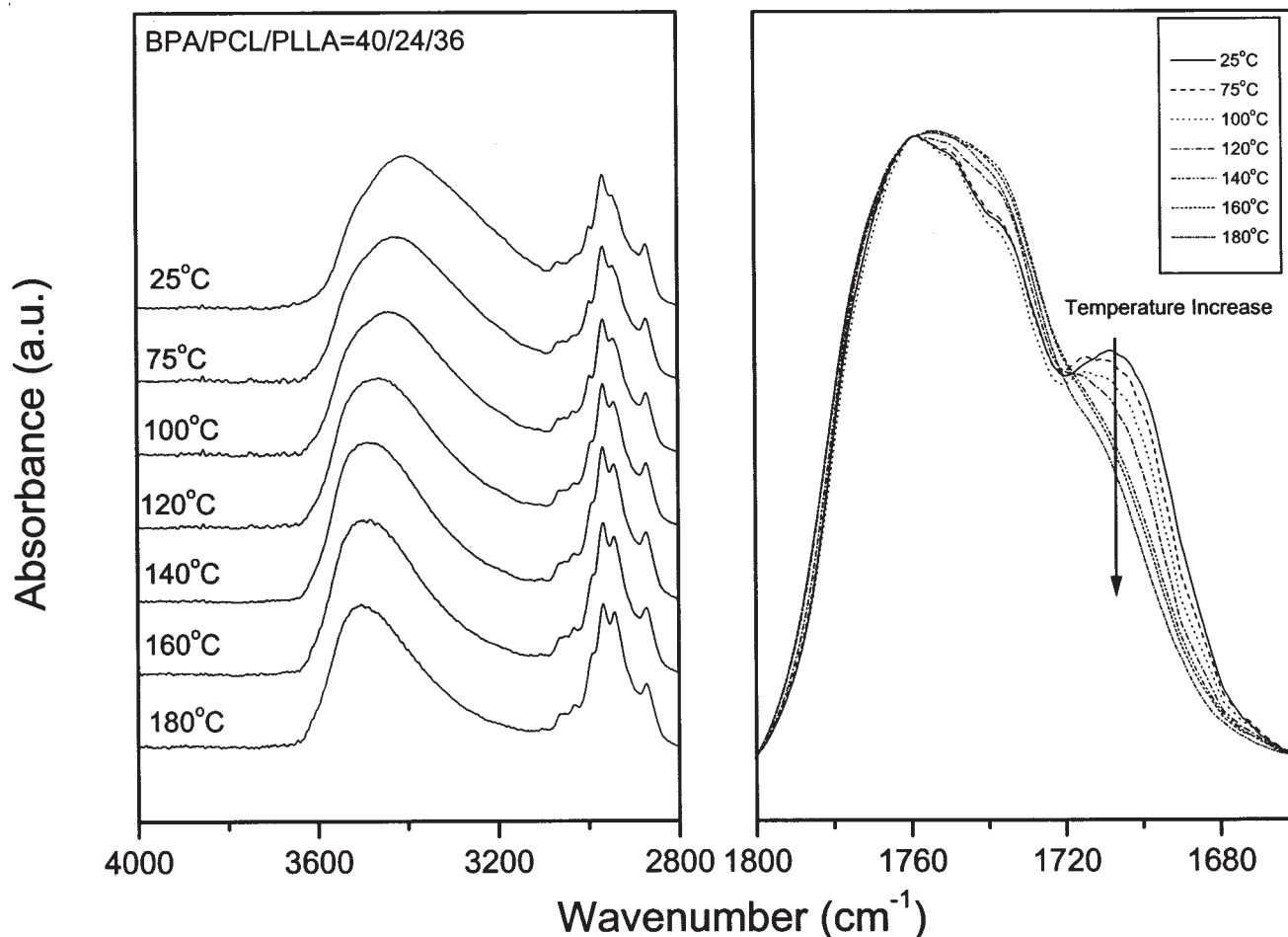


**Figure 15** FTIR spectra recorded at various temperatures displaying the (a) hydroxyl and (b) carbonyl group stretching regions for the blend BPA/PCL/PLLA = 40/24/36.

should arise from the BPA phase. In contrast, two values of  $T_g$  are also observed at 60 wt % BPA. These two  $T_g$ 's are close to one another, however, and become indistinguishable in comparison with that observed at lower BPA content (as shown in Fig. 5). Figure 10 shows corresponding optical micrographs of the BPA/PCL/PLLA system at constant BPA contents (60 and 80 wt %): it appears that both the binary and ternary blends are homogeneous, which indicates that these blends are totally miscible. The different results obtained from the DSC and OM analyses at a BPA content of 60 wt % content arise because of the different resolutions expected from each measurement.

In general, DSC discriminates between situations in which there are either one or two values of  $T_g$ : a single value of  $T_g$  is the most convenient criterion for determining the miscibility of a polymer blend. In contrast, an immiscible polymer blend exhibits more than one value of  $T_g$ . A single compositionally dependent glass transition indicates full miscibility at dimensions on the order of 20–40 nm, whereas optical transparency in an OM analysis indicates miscibility dimensions on the order of

only ca.1  $\mu\text{m}$ . As a result, in some cases, a film that appears homogeneous by OM analysis may have two values of  $T_g$  when analyzed by DSC. The carbonyl group stretching region (1660–1800  $\text{cm}^{-1}$ ) of the infrared spectra of these ternary blends measured at 180°C are presented in Figure 11. The three major absorptions for carbonyl group stretching are similar to those displayed in Figure 8 and the results of curve fitting from Gaussian functions are also summarized in Table V. The fraction of hydrogen-bonded carbonyl group of PCL is decreased with increasing the PLLA content, which indicates that the hydrogen bonding interaction exists between the hydroxyl groups of BPA and the carbonyl groups of both PCL and PLLA. As a result, the immiscible BPA/PCL/PLLA blend tends to become a miscible ternary blend at relatively higher BPA content.

Using OM to observe phase morphologies of BPA/PCL/PLLA ternary blends with respect to temperatures

We examined the effect that temperature has on the phase transition (from phase separation to miscibility

upon heating) in the immiscible ternary blends, using OM with a heating stage. Figure 12 shows optical micrographs recorded at various temperatures of several selected ternary blend compositions having relatively low BPA content (20 and 40 wt %). The phase separation domain of these ternary blend compositions disappeared with the increasing the temperature, which indicates that an upper critical solution temperatures (UCST) phase diagram exists at lower BPA content. However, at higher BPA content, a homogeneous single phase was observed at all measured temperatures (for brevity, the images are not shown here). In addition, the binary PCL/PLLA blend also exhibits UCST phase diagram. Figure 13 summarizes the phase diagrams of the ternary blends at different temperatures based on the OM analyses. At 40°C, the addition of a large BPA content (>60 wt %) cause the binary PCL/PLLA blend to become miscible. At 140°C, the miscibility window become a closed-loop phase diagram, which is similar to the situations observed for phenolic/PEO/PCL, phenoxy/PMMA/PEO, and SAA/PMMA/PEO ternary blends.<sup>48–50</sup> In addition, the phase diagram becomes totally miscible at 200°C, which has also been observed in previous studies.<sup>51–54</sup> The enhancement of the miscibility observed in this ternary BPA/PCL/PLLA system at lower BPA content is caused by the rapid decrease of the interassociation equilibrium constant of the BPA/PCL blend (higher interassociation enthalpy)<sup>55</sup> upon the increasing the temperature; the  $\Delta K$  and effects are balanced at higher temperature as presented in Figure 14. Therefore, the  $\Delta K$  effect becomes smaller at higher temperature. A large entropy change dominates at higher temperature, and thus, miscibility is enhanced. Figure 15 provides evidence that the fraction of hydrogen-bonded carbonyl group of PCL (b) and the average strength of hydrogen bonding (a) decreases upon increase in temperature.

## CONCLUSIONS

The addition of BPA enhances the miscibility of the immiscible binary PCL/PLLA blend and eventually transforms it into a completely miscible blend having a single value of  $T_g$  when a sufficiently large amount of BPA is present. The interassociation equilibrium constant between the hydroxyl group of BPA and the carbonyl groups of PCL is higher than that for the corresponding interaction with the carbonyl groups of PLLA. This result implies that the tendency to forming hydrogen bonds between BPA and PCL is more favorable than the interassociation of BPA with PLLA. OM measurements indicate an UCST phase diagram, since the  $\Delta K$  effect becomes smaller as temperatures increase above room temperature.

## References

- Ha, C. K.; Cho, W. *J Prog Polym Sci* 2002, 27, 759.
- Reeve, M. S.; McCathy, S. P.; Downey, M. J.; Gross, R. A. *Macromolecules* 1994, 27, 825.
- Kikkawa, Y.; Abe, H.; Iwata, T.; Doi, Y. *Biomacromolecules* 2001, 2, 940.
- Eastmond, G. C. *Adv Polym Sci* 1999, 149, 223.
- Li, S.; Liu, L.; Garreau, H.; Vert, M. *Biomacromolecules* 2003, 4, 372.
- Hiljanen-Vainio, M.; Varpomaa, P.; Seppala, J.; Tormala, P. *Macromol Chem Phys* 1996, 197, 1503.
- Yang, J. M.; Chen, H. L.; You, J. W.; Hwang, J. C. *Polym J* 1997, 29, 657.
- Wang, L.; Ma, W.; Gross, R. A.; McCathy, S. P. *Polym Degrad Stab* 1998, 59, 161.
- Dell'Erba, T.; Groeninckx, G.; Maglio, G.; Malinconico, M.; Migliozi, A. *Polymer* 2001, 42, 7831.
- Tsuji, H.; Yamada, T.; Suzuki, M.; Itsuno, S. *Polym Int* 2003, 52, 269.
- Maglio, G.; Migliozi, A.; Palumbo, R.; Immirzi, B.; Volpe, M. G. *Macromol Rapid Commun* 1999, 20, 236.
- Choi, N. S.; Kim, C. H.; Cho, K. Y.; Park, J. K. *J Appl Polym Sci* 2002, 86, 1892.
- Kim, C. H.; Cho, K. Y.; Choi, E. J.; Park, J. K. *J Appl Polym Sci* 2000, 77, 226.
- Na, Y. H.; He, Y.; Shuai, X.; Kikkawa, Y.; Doi, Y.; Inoue, Y. *Biomacromolecules* 2002, 3, 1179.
- Scott, R. L. *J Chem Phys* 1949, 17, 279.
- Tompa, H. *Trans Faraday Soc* 1949, 45, 1142.
- Pomposo, J. A.; Calahorra, E.; Eguiazabal, I.; Cortazar, M. *Macromolecules* 1993, 26, 2104.
- Kwei, T. K.; Frisch, H. L.; Radigan, W.; Vogel, S. *Macromolecules* 1977, 10, 157.
- Kuo, S. W.; Huang, C. F.; Chang, F. C. *J Polym Sci Part B: Polym Phys* 2001, 39, 1389.
- Kuo, S. W.; Chan, S. C.; Chang, F. C. *Macromolecules* 2003, 36, 6653.
- Chen, H. L.; Liu, H. H.; Lin, J. S. *Macromolecules* 2000, 33, 4856.
- Zhang, L. L.; Goh, S. H.; Lee, S. Y. *J Appl Polym Sci* 1998, 70, 1811.
- Zhang, L. L.; Goh, S. H.; Lee, S. Y. *Polymer* 1998, 39, 4841.
- Koning, C.; Van-Duin, M.; Pagnoulle, C.; Jerome, R. *Prog Polym Sci* 1998, 23, 707.
- He, Y.; Asakawa, N.; Inoue, Y. *Macromol Chem Phys* 2001, 202, 1035.
- He, Y.; Asakawa, N.; Inoue, Y. *J Polym Sci Part B: Polym Phys* 2000, 38, 1848.
- He, Y.; Asakawa, N.; Inoue, Y. *J Polym Sci Part B: Polym Phys* 2000, 38, 2891.
- Li, J.; He, Y.; Inoue, Y. *J Polym Sci Part B: Polym Phys* 2001, 39, 2108.
- Li, J.; He, Y.; Ishida, K.; Yamane, T.; Inoue, Y. *Polym J* 2001, 33, 773.
- He, Y.; Asakawa, N.; Li, J.; Inoue, Y. *J Appl Polym Sci* 2001, 82, 640.
- Watanabe, T.; He, Y.; Asakawa, N.; Yoshie, N.; Inoue, Y. *Polym Int* 2001, 50, 463.
- Kuo, S. W.; Chan, S. C.; Chang, F. C. *Polymer* 2002, 43, 3653.
- Li, D. X.; Goh, S. H. *J Polym Sci Part B: Polym Phys* 2001, 39, 1815.
- Li, D. X.; Goh, S. H. *J Appl Polym Sci* 2001, 81, 901.
- Li, D. X.; Goh, S. H. *J Polym Sci Part B: Polym Phys* 2002, 40, 1125.
- Li, D. X.; Goh, S. H. *Polymer* 2002, 43, 6853.
- Li, D. X.; Goh, S. H.; Zheng, J. W. *J Appl Polym Sci* 2003, 87, 1137.

38. Li, D. X.; Goh, S. H. *Macromol Chem Phys* 2002, 203, 2334.
39. Kwei, T. K. *J Polym Sci Polym Lett Ed* 1984, 22, 307.
40. Li, X. D.; Goh, S. H. *J Polym Sci Polym Phys Ed* 2003, 41, 789.
41. Kuo, S. W.; Chang, F. C. *Macromol Chem Phys* 2002, 202, 868.
42. Wu, H. D.; Chu, P. P.; Ma, C. C. M.; Chang, F. C. *Macromolecules* 1999, 32, 3097.
43. Moskala, E. J.; Varnell, D. F.; Coleman, M. M. *Polymer* 1985, 26, 228.
44. Coleman, M. M.; Graf, J. F.; Painter, P. C. *Specific Interactions and the Miscibility of Polymer Blends*; Technomic Publishing: Lancaster, PA, 1991.
45. Coleman, M. M.; Painter, P. C. *Prog Polym Sci* 1995, 20, 1.
46. Zhang, H.; Bhagwagar, D. E.; Graf, J. F.; Painter, P. C.; Coleman, M. M. *Polymer* 1994, 35, 5379.
47. Coleman, M. M.; Yang, X.; Painter, P. C.; Graf, J. F. *Macromolecules* 1992, 25, 4414.
48. Kuo, S. W.; Lin, C. L.; Chang, F. C. *Macromolecules* 2002, 35, 278.
49. Hong, B. K.; Kim, J. K.; Jo, W. H.; Lee, S. C. *Polymer* 1997, 38, 4373.
50. Jo, W. H.; Kwon, Y. K.; Kwon, I. H. *Macromolecules* 1991, 24, 4708.
51. Min, K. E.; Chiou, J. S.; Barlow, J. W.; Paul, D. R. *Polymer* 1987, 28, 172.
52. Guo, Q. P. *Eur Polym J* 1996, 32, 1409.
53. Guo, Q. P. *Eur Polym J* 1990, 26, 1329.
54. Goh, S. H.; Ni, X. *Polymer* 1999, 40, 5733.
55. Kuo, S. W.; Chang, F. C. *Macromolecules* 2001, 34, 4089.